Supplemental Figures

Targeting Pancreatic Cancer by TAK-981, a SUMOylation Inhibitor that Activates the Immune System and Blocks Cancer Cell Cycle Progression in a Preclinical Model

Sumit Kumar[1], Mark J.A. Schoonderwoerd[2], Jessie S. Kroonen[1], Ilona J. de Graaf[1], Marjolein Sluijter[3], Dina Ruano[4], Román González-Prieto[1], Matty Verlaan–de Vries[1], Jasper Rip[5], Ramon Arens[5], Noel F.C.C. de Miranda[4], Lukas J.A.C. Hawinkels[2§], Thorbald van Hall[3§], Alfred C.O. Vertegaal[1*]

[1]Cell and Chemical Biology, Leiden University Medical Center, 2333, ZA, Leiden, the Netherlands.

[2]Gastroenterology and Hepatology, Leiden University Medical Center, 2333, ZA, Leiden, the Netherlands.

[3]Medical Oncology, Oncode Institute, Leiden University Medical Center, 2333, ZA, Leiden, the Netherlands.

[4]Pathology, Leiden University Medical Center, 2333, ZA, Leiden, the Netherlands.

[5]Immunology, Leiden University Medical Center, 2333, ZA, Leiden, the Netherlands.

[§]equal contributors

*Email: vertegaal@lumc.nl

Kumar S, *et al. Gut* 2022; 71:2266–2283. doi: 10.1136/gutjnl-2021-324834

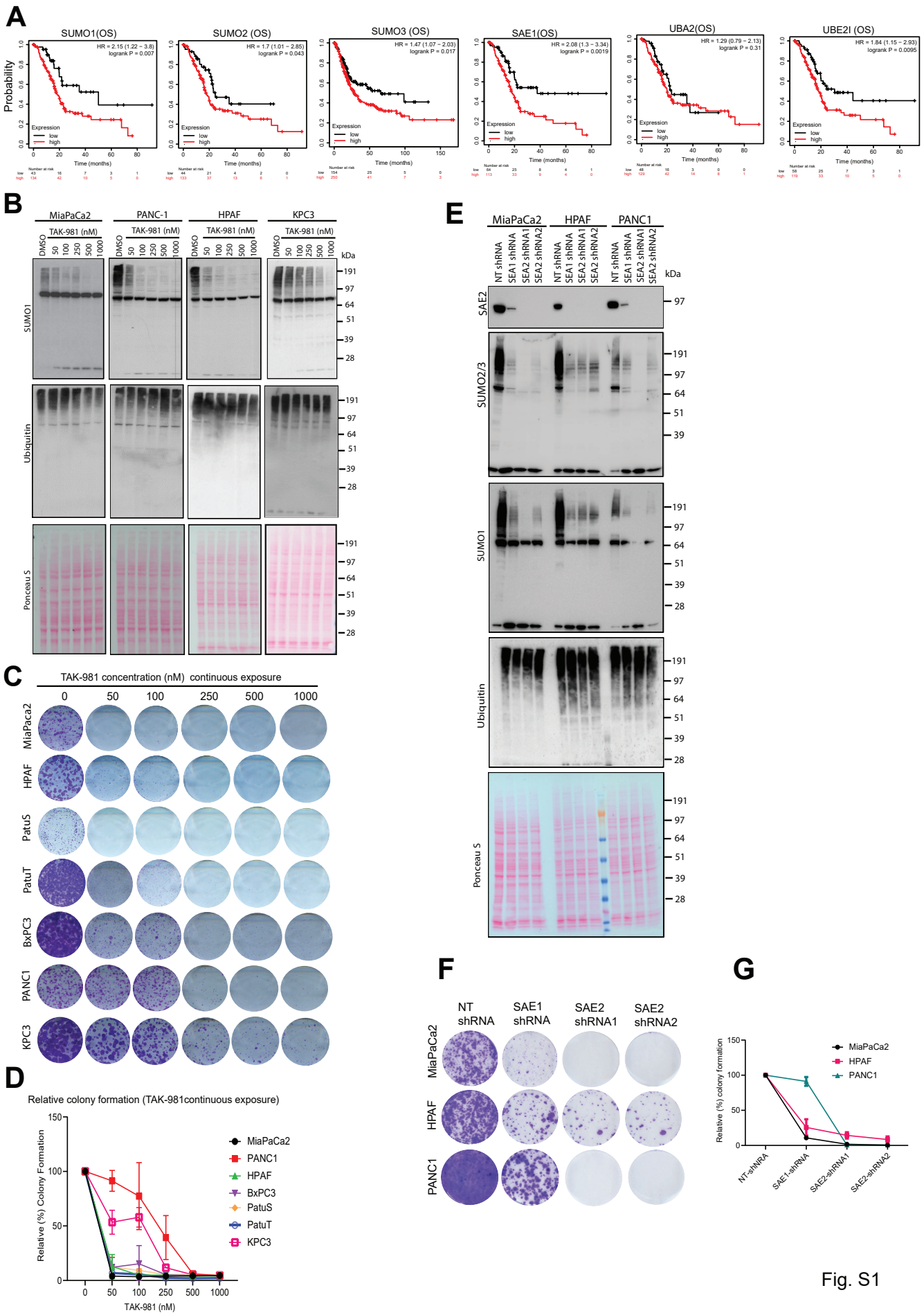
A
SUMO1(OS)
SUMO2 (OS)
SUMO3 (OS)
SAE1(OS)
UBA2(OS)
UBE2I (OS)
Probability
Expression
low
high
Time (months)
B
MiaPaCa2
PANC-1
HPAF
KPC3
TAK-981 (nM)
DMSO
50
100
250
500
1000
kDa
SUMO1
Ubiquitin
Ponceau S
191
97
64
51
39
28
C
TAK-981 concentration (nM) continuous exposure
0
50
100
250
500
1000
MiaPaCa2
HPAF
PatuS
PatuT
BxPC3
PANC1
KPC3
D
Relative colony formation (TAK-981continuous exposure)
Relative (%) Colony Formation
TAK-981 (nM)
MiaPaCa2
PANC1
HPAF
BxPC3
PatuS
PatuT
KPC3
E
MiaPaCa2
HPAF
PANC1
NT shRNA
SEA1 shRNA
SEA2 shRNA1
SEA2 shRNA2
kDa
SAE2
SUMO2/3
SUMO1
Ubiquitin
Ponceau S
F
NT shRNA
SAE1 shRNA
SAE2 shRNA1
SAE2 shRNA2
MiaPaCa2
HPAF
PANC1
G
Relative (%) colony formation
MiaPaCa2
HPAF
PANC1
NT-shRNA
SAE1-shRNA
SAE2-shRNA1
SAE2-shRNA2

Fig. S1

Figure S1. TAK-981 treatment and SUMO E1 knockdown block SUMO pathway activity and proliferation.

(A) Kaplan-Meier plots showing overall survival of PDAC patients with high or low SUMO pathway gene expression. Patients with expression above the median are indicated in red lines, and patients with expression below the median are indicated in black lines. HR represents hazard ratio. The p-values are derived by log-rank tests.

(B) Western blot analysis of SUMO1 and ubiquitin levels in MiaPaCa2, PANC1, HPAF and KPC3, treated for 4 h with the indicated concentrations of TAK-981. Ponceau S staining was used as loading control.

(C) Human pancreatic cancer cell lines MiaPaCa2, PANC1, HPAF, BxPC3, PatuS, PatuT and mouse pancreatic cell line KPC3 were treated with the indicated concentrations of TAK-981 for 10 days and colony formation was determined by crystal violet staining.

(D) Line graphs represent the absorbance of solubilized crystal violet as mean with standard deviation (n=3).

(E) Knockdown of the SUMO-activating enzyme (SAE) in pancreatic cells MiaPaCa2, PANC1 and HPAF was carried out by stably expressing doxycycline inducible shRNAs generated against both SAE subunits SAE1 (SAE1 shRNA) and SAE2 (SAE2 shRNA1 and 2). Scrambled shRNA was used as a control (NT shRNA). Cells were treated with 100 ng/ml doxycycline for 4 days. Protein lysates were immunoblotted with SUMO2/3, SUMO1 and ubiquitin antibodies. Ponceau S staining was used as loading control.

(F) MiaPaCa2, PANC1 and HPAF cells stably expressing doxycycline inducible SAE knockdown constructs were plated at low density in 6 well plates. Cells were treated

with 100 ng/ml doxycycline for 10 days. Colony formation was determined by crystal violet staining.

(G) Line graphs represent the absorbance of solubilized crystal violet. Error bars denote standard deviation (n=4). Data related to Fig. 1.

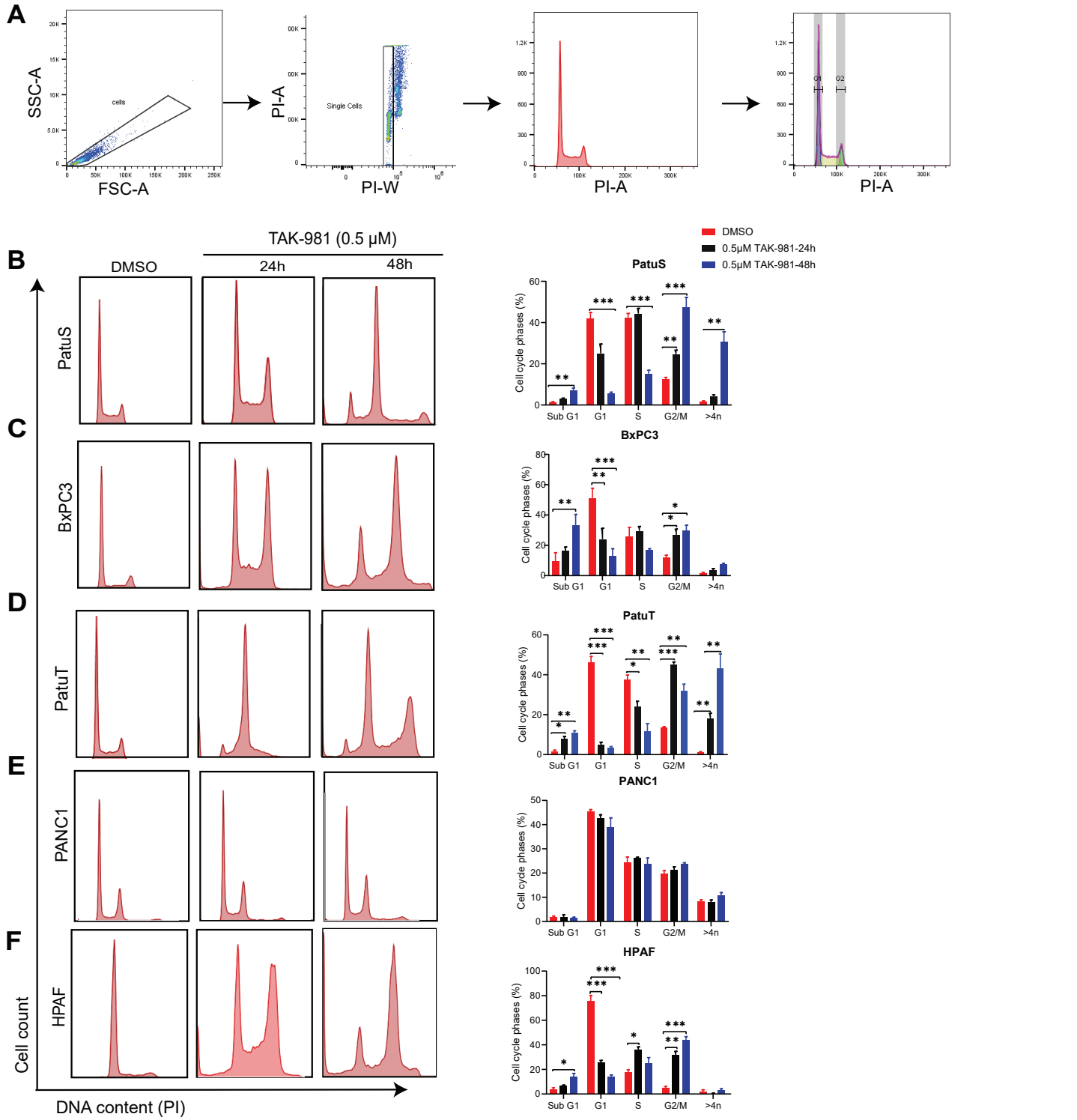
A
SSC-A
FSC-A
cells
PI-A
PI-W
Single Cells
PI-A
G1
G2
PI-A
B
C
D
E
F
TAK-981 (0.5 μM)
DMSO
24h
48h
PatuS
BxPC3
PatuT
PANC1
HPAF
Cell count
DNA content (PI)
DMSO
0.5μM TAK-981-24h
0.5μM TAK-981-48h
Cell cycle phases (%)
Sub G1
G1
S
G2/M
>4n
G
MiaPaCa2
HPAF
BxPC3
PatuS
PatuT
PANC1
DMSO
24h
48h
TAK-981
kDa
191
97
64
SUMO2/3
ponceau S
H
MiaPaca2
DMSO
0.5 μM TAK-981
cells with micronuclei (%)
DMSO
TAK-981

Fig. S2

Figure S2. Cell cycle analysis after TAK-981 treatment.

(A) Gating strategy for cell cycle analysis upon TAK-981 treatment.

(B-F) Cell cycle analysis of PANC1, HPAF, BxPC3, PatuS, PatuT after 0.5 μM TAK-981 or 0.1% DMSO for 24 h and 48 h. Cellular DNA content was determined by propidium iodide staining and flowcytometry. Bar graphs showing the percentage of cells in each cell cycle phase (G1, S, G2/M and >4n) of three biological replicates (*n*=3). Error bars represent SEM and p-values are derived from two-sided two sample t-tests. *p < 0.05; **p < 0.01; ***p < 0.001; ****p < 0.0001.

(G) Western blot analysis of SUMO2/3 levels in lysates of MiaPaCa2, HPAF, BxPC3, PatuS, PatuT and PANC1 treated for 24 h and 48 h with TAK-981. Ponceau S staining was used as loading control.

(H) Untreated or 0.5 μM TAK-981 treated MiaPaCa2 cells were fixed and stained with DAPI. The percentage of nuclei associated with one or more micronuclei are shown. More than 1000 cells were counted from two independent biological replicates. The bar graph shows the average percentage of cells that were associated with micronuclei. Error bars represent standard deviations and the *p* -value is derived from a two-sided two-sample *t*-test with n=2 independent experiments. *p < 0.05; **p < 0.01; ***p < 0.001; ****p < 0.0001. Representative micrographs are shown. Scale bars represent 10 μm. Data related to Fig. 2.

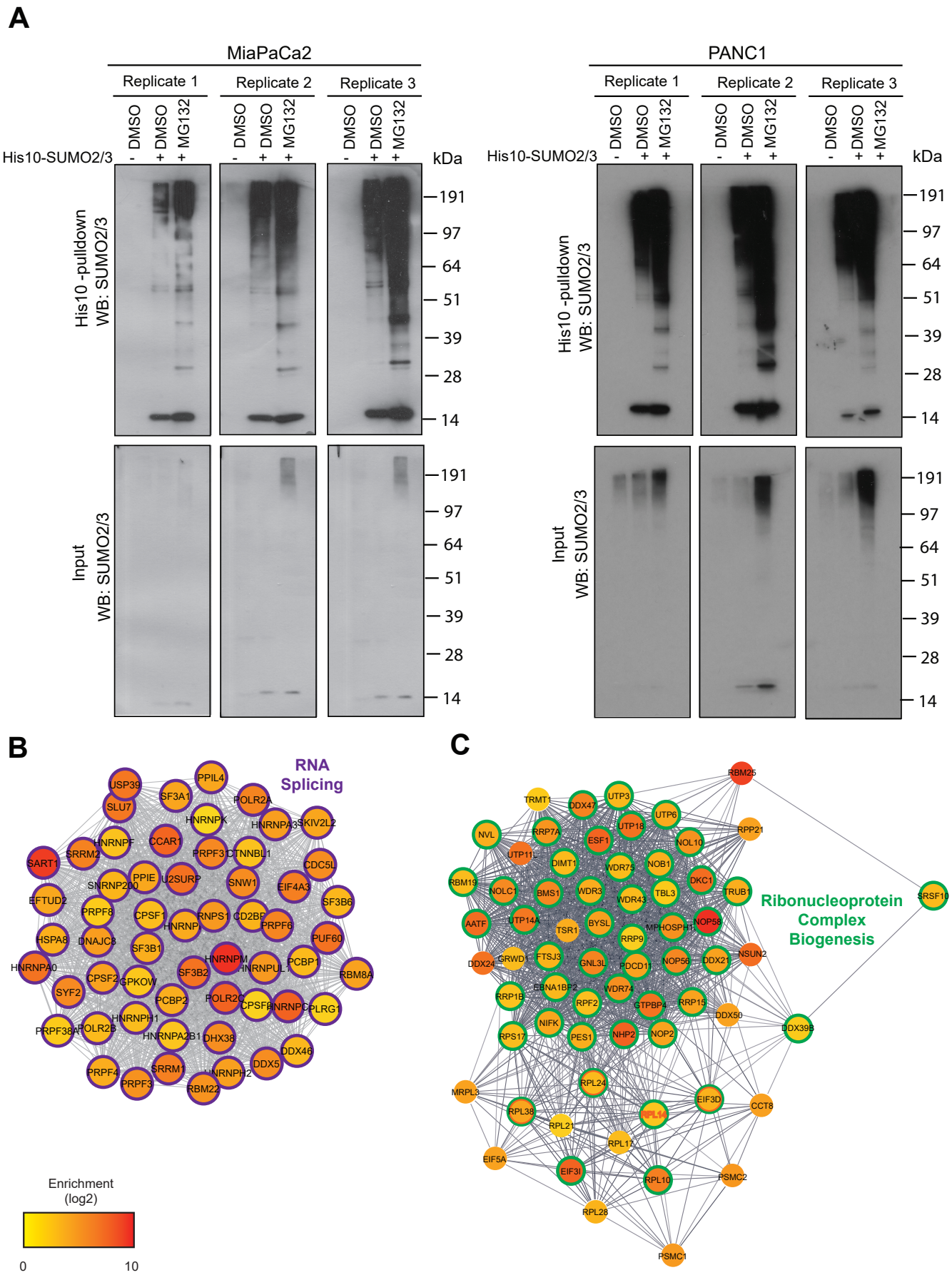
A
MiaPaCa2
PANC1
Replicate 1
Replicate 2
Replicate 3
- DMSO
+ DMSO
+ MG132
His10-SUMO2/3
kDa
191
97
64
51
39
28
14
His10 -pulldown WB: SUMO2/3
Input WB: SUMO2/3
B
RNA Splicing
USP39
PPIL4
SF3A1
POLR2A
SLU7
HNRNPK
HNRNPA3
KIV2L2
HNRNPF
CCAR1
SRRM2
PRPF3
CTNNBL1
SART1
CDC5L
PPIE
U2SURP
SNW1
EIF4A3
SNRNP200
EFTUD2
PRPF8
CPSF1
SF3B6
HNRNP
RNPS1
CD2BP2
PRPF6
HSPA8
DNAJC8
PUF60
SF3B1
HNRNPM
HNRNPA0
HNRNPUL1
PCBP1
CPSF2
SF3B2
RBM8A
GPKOW
SYF2
PCBP2
POLR2C
CPSF6
HNRNPC
PLRG1
HNRNPH1
PRPF38A
POLR2B
HNRNPA2B1
DHX38
DDX46
PRPF4
SRRM1
DDX5
HNRNPH2
PRPF3
RBM22
Enrichment (log2)
0
10
C
Ribonucleoprotein Complex Biogenesis
RBM25
TRMT1
DDX47
UTP3
UTP6
NVL
RRP7A
ESF1
UTP18
RPP21
NOL10
UTP11L
DIMT1
WDR75
NOB1
RBM19
NOLC1
BMS1
WDR3
WDR43
TBL3
DKC1
TRUB1
SRSF10
AATF
UTP14A
TSR1
BYSL
RRP9
MPHOSPH10
NOP58
DDX24
SRWD1
FTSJ3
GNL3L
PDCD11
NOP56
DDX21
NSUN2
EBNA1BP2
WDR74
RRP1B
RPF2
GTPBP4
RRP15
DDX50
DDX39B
NIFK
RPS17
PES1
NHP2
NOP2
MRPL3
RPL24
EIF3D
CCT8
RPL38
RPL10
RPL21
RPL17
EIF5A
EIF3I
RPL10
PSMC2
RPL28
PSMC1

Fig. S3

Figure S3. **Analysis of SUMO2/3 target proteins in pancreatic cancer cell lines.**

(A) Immunoblot analysis of three replicates of MiaPaCa2 and PANC1 analyzed by LC-MS/MS. SUMO2/3 antibody was used to confirm efficient enrichment of SUMO conjugated proteins.

(B-C) STRING network analysis of SUMO2/3 target proteins. Clusters contain multiple proteins involved in RNA splicing and ribonucleoprotein complex biogenesis. Data related to Fig. 2.

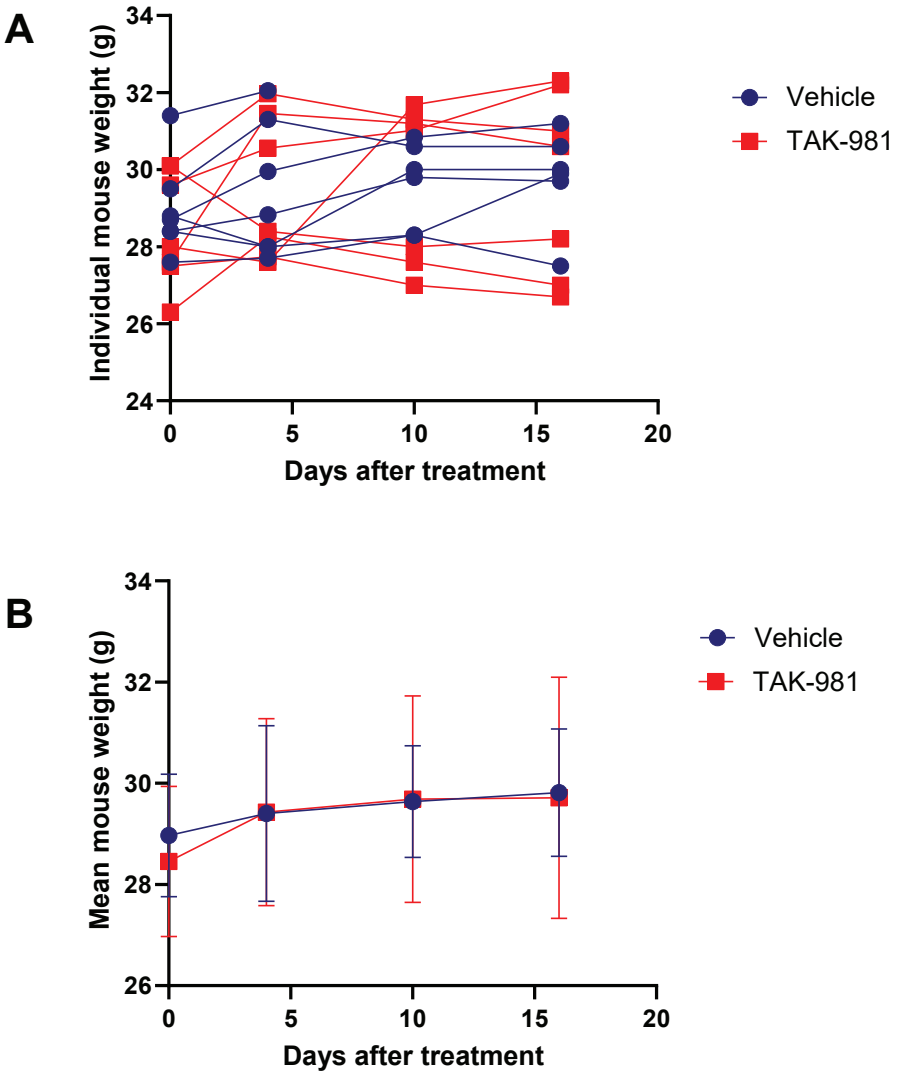
A
Individual mouse weight (g)
34
32
30
28
26
24
0
5
10
15
20
Days after treatment
Vehicle
TAK-981
B
Mean mouse weight (g)
34
32
30
28
26
0
5
10
15
20
Days after treatment
Vehicle
TAK-981

Fig. S4

Figure S4. TAK-981 is well tolerated by mice.

(A-B) C57BL/6 mice bearing KPC3 tumors were treated twice weekly with 7.5 mg/kg TAK-981 or solvent. Mice weight was monitored twice a week during treatment. Both mean and individual mouse weights are shown. Data related to Fig. 3.

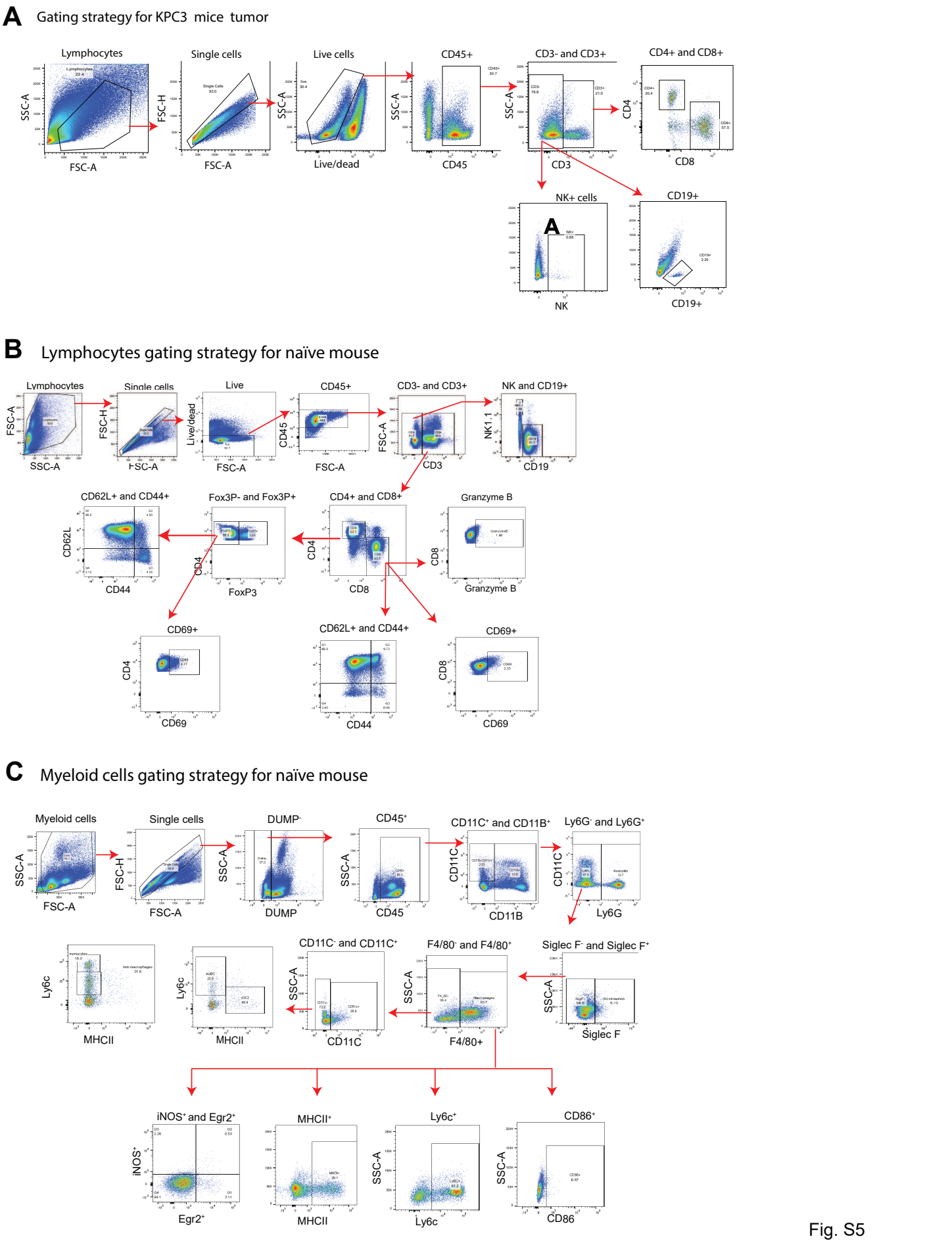
A
Gating strategy for KPC3 mice tumor
Lymphocytes
Single cells
Live cells
CD45+
CD3- and CD3+
CD4+ and CD8+
NK+ cells
CD19+
B
Lymphocytes gating strategy for naïve mouse
CD62L+ and CD44+
Fox3P- and Fox3P+
CD4+ and CD8+
Granzyme B
CD69+
C
Myeloid cells gating strategy for naïve mouse
Myeloid cells
Single cells
DUMP-
CD45+
CD11C+ and CD11B+
Ly6G- and Ly6G+
CD11C- and CD11C+
F4/80- and F4/80+
Siglec F- and Siglec F+
iNOS+ and Egr2+
MHCII+
Ly6c+
CD86+

Fig. S5

Figure S5. Gating strategy for flow cytometry analysis.

(A) Gating strategy for flow cytometry analysis of lymphocytes from the KPC3 tumor samples.

(B) Gating strategy for the flow cytometry analysis of lymphocytes from peripheral blood, lymph nodes, spleen and bone marrow of naïve mice.

(C) Gating strategy for the flow cytometry analysis of myeloid cells from peripheral blood, lymph nodes, spleen and bone marrow of naïve mice. Data related to Fig. 4.

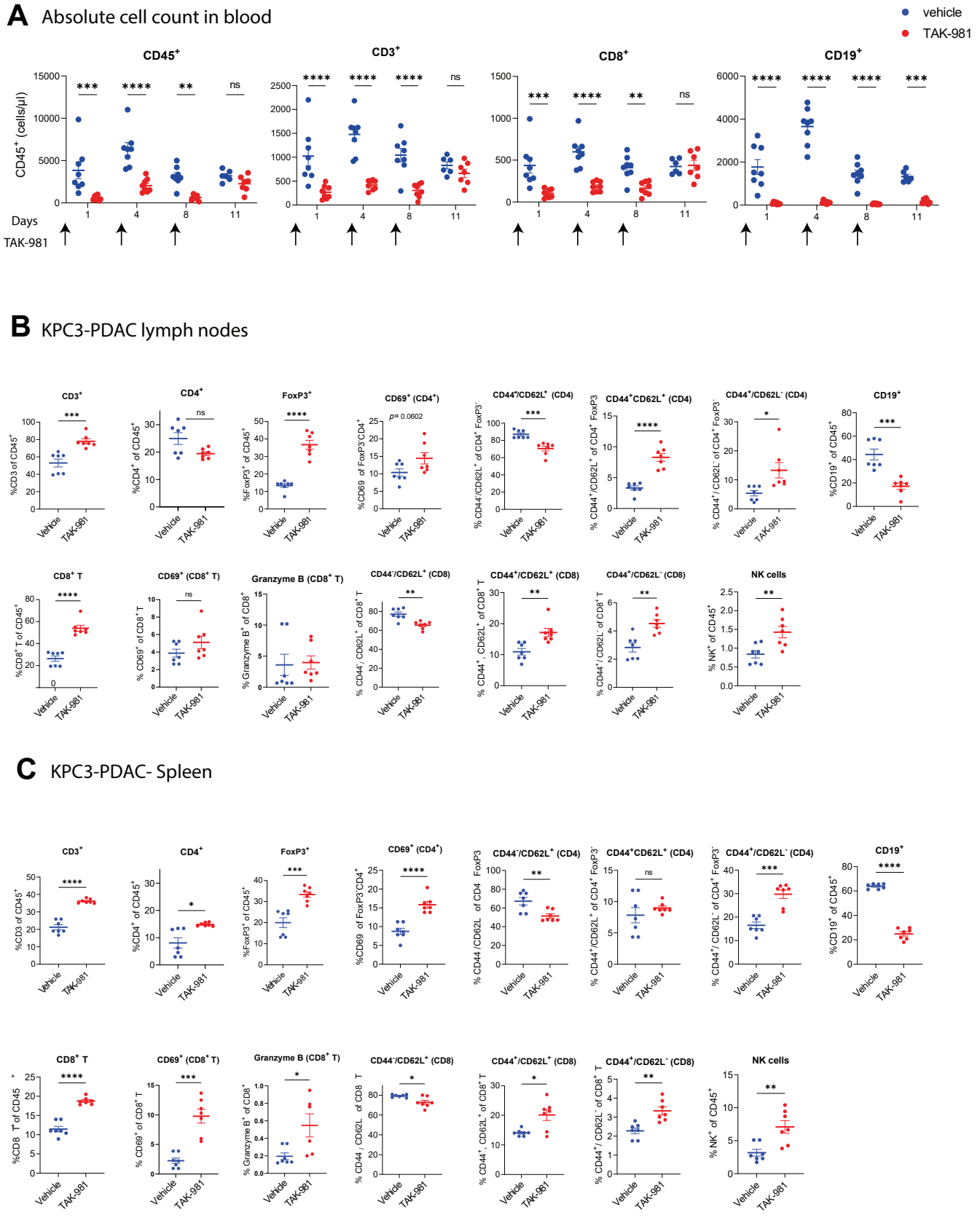
A Absolute cell count in blood
vehicle
TAK-981
CD45+
CD3+
CD8+
CD19+
CD45+ (cells/µl)
Days
TAK-981
B KPC3-PDAC lymph nodes
CD3+
CD4+
FoxP3+
CD69+ (CD4+)
CD44+/CD62L+ (CD4)
CD44+CD62L+ (CD4)
CD44+/CD62L- (CD4)
CD19+
CD8+ T
CD69+ (CD8+ T)
Granzyme B (CD8+ T)
CD44-/CD62L+ (CD8)
CD44+/CD62L+ (CD8)
CD44+/CD62L- (CD8)
NK cells
C KPC3-PDAC- Spleen
Vehicle
TAK-981

Fig. S6

Figure S6. Flow cytometry analysis to monitor immune modulation by TAK-981 in KPC3 tumor bearing mice.

(A) KPC3 tumor bearing C57BL/6 mice were treated with TAK-981 or vehicle control at days 0, 3, 7 and blood was harvested on days 1, 4, 8, 11. Absolute cell counts were determined using counting beads. **(B)** Lymph nodes **(C)** Spleen. Graphs represent mean and SEM. Statistical testing was performed using two way ANOVA with Sidak's multiple comparison test. *p < 0.05; **p < 0.01; ***p < 0.001; ****p < 0.0001. Data related to Fig. 4.

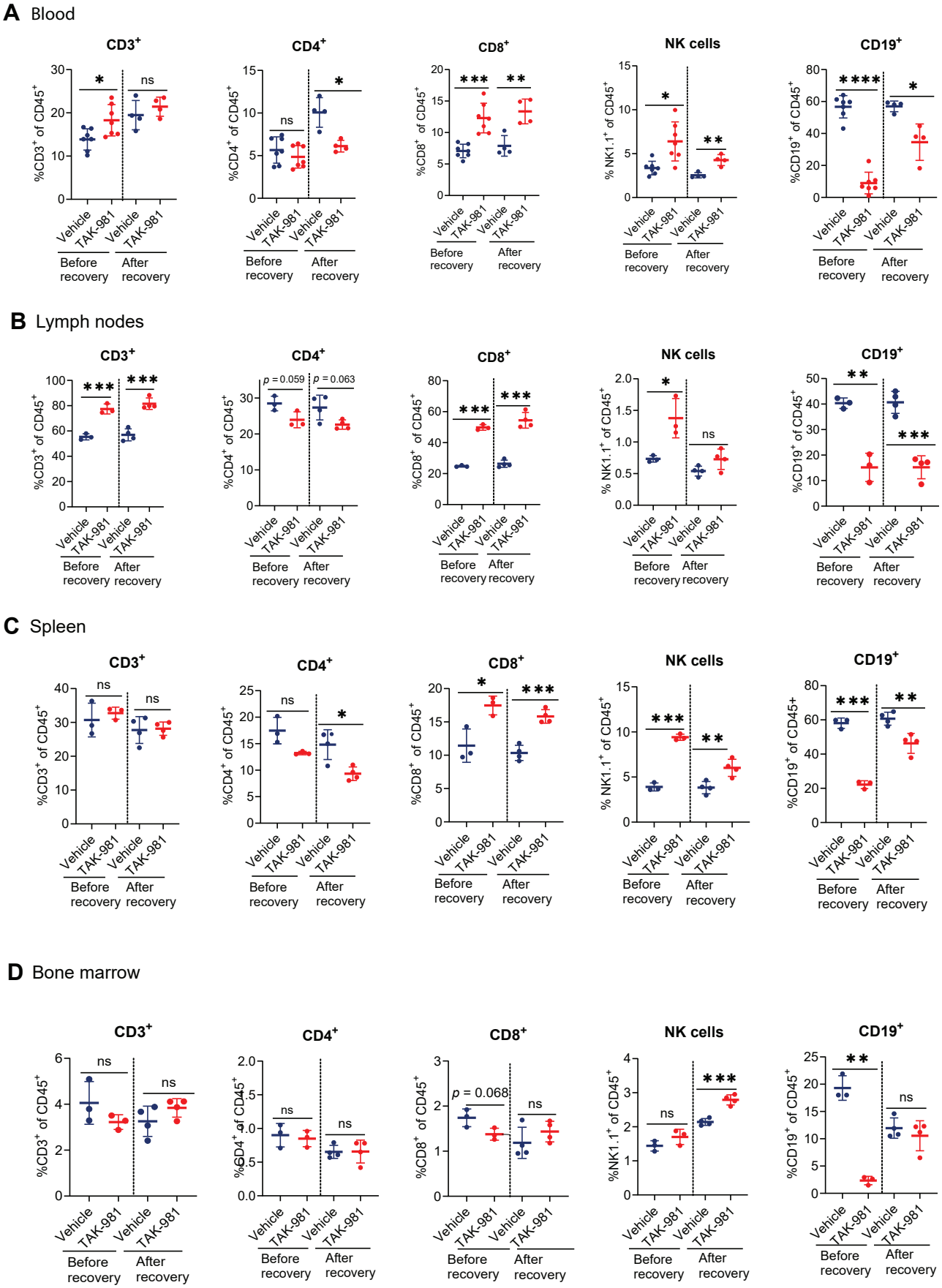
A Blood
B Lymph nodes
C Spleen
D Bone marrow
CD3+
CD4+
CD8+
NK cells
CD19+
%CD3+ of CD45+
%CD4+ of CD45+
%CD8+ of CD45+
% NK1.1+ of CD45+
%CD19+ of CD45+
p = 0.059
p = 0.063
p = 0.068
ns
Vehicle
TAK-981
Before recovery
After recovery

Fig. S7

Figure S7. Flow cytometry analysis of lymphocytes from naïve mice.

(A-D) Flow cytometry analysis of lymphocytes from **(A)** blood, **(B)** lymph nodes, **(C)**spleen and **(D)** bone marrow. C57BL/6 naïve mice were injected with either vehicle or 7.5 mg/kg TAK-981 twice a week on days 0, 3, 7, 10. Blood was collected on days 1, 4, 8, 11, 15 from the treated mice. Graphs represent mean and SD. Statistical testing was performed using unpaired two-tailed Welch's t test. *$p < 0.05$; **$p < 0.01$; ***$p < 0.001$; ****$p < 0.0001$. Data related to Fig. 4.

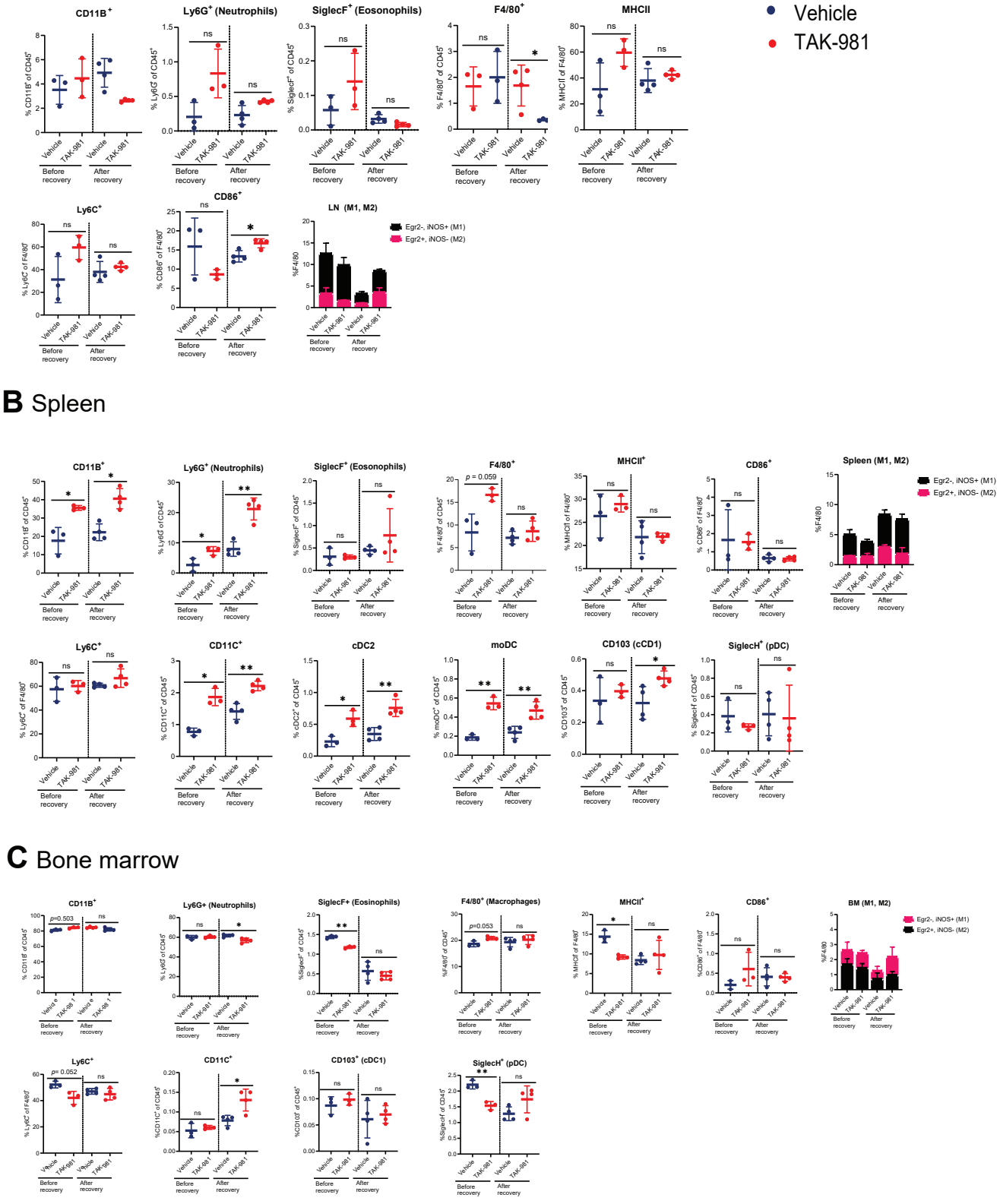
A Lymph nodes
B Spleen
C Bone marrow
Vehicle
TAK-981
CD11B+
Ly6G+ (Neutrophils)
SiglecF+ (Eosonophils)
F4/80+
MHCII
Ly6C+
CD86+
LN (M1, M2)
Egr2-, iNOS+ (M1)
Egr2+, iNOS- (M2)
CD11C+
cDC2
moDC
CD103 (cCD1)
SiglecH+ (pDC)
Spleen (M1, M2)
Ly6G+ (Neutrophils)
SiglecF+ (Eosinophils)
F4/80+ (Macrophages)
CD103+ (cDC1)
BM (M1, M2)
Before recovery
After recovery
ns

Fig. S8

Figure S8. Flow cytometry analysis of myeloid cells.

(A-C) Flow cytometry analysis of myeloid cells from **(A)** lymph nodes, **(B)** spleen and **(C)** bone marrow. Graphs represent mean and SD. Statistical testing was performed using unpaired two-tailed Welch's t test. *p < 0.05; **p < 0.01; ***p < 0.001; ****p < 0.0001. Data related to Fig. 4.

Gating strategy for B cell sub-types analysis in spleen

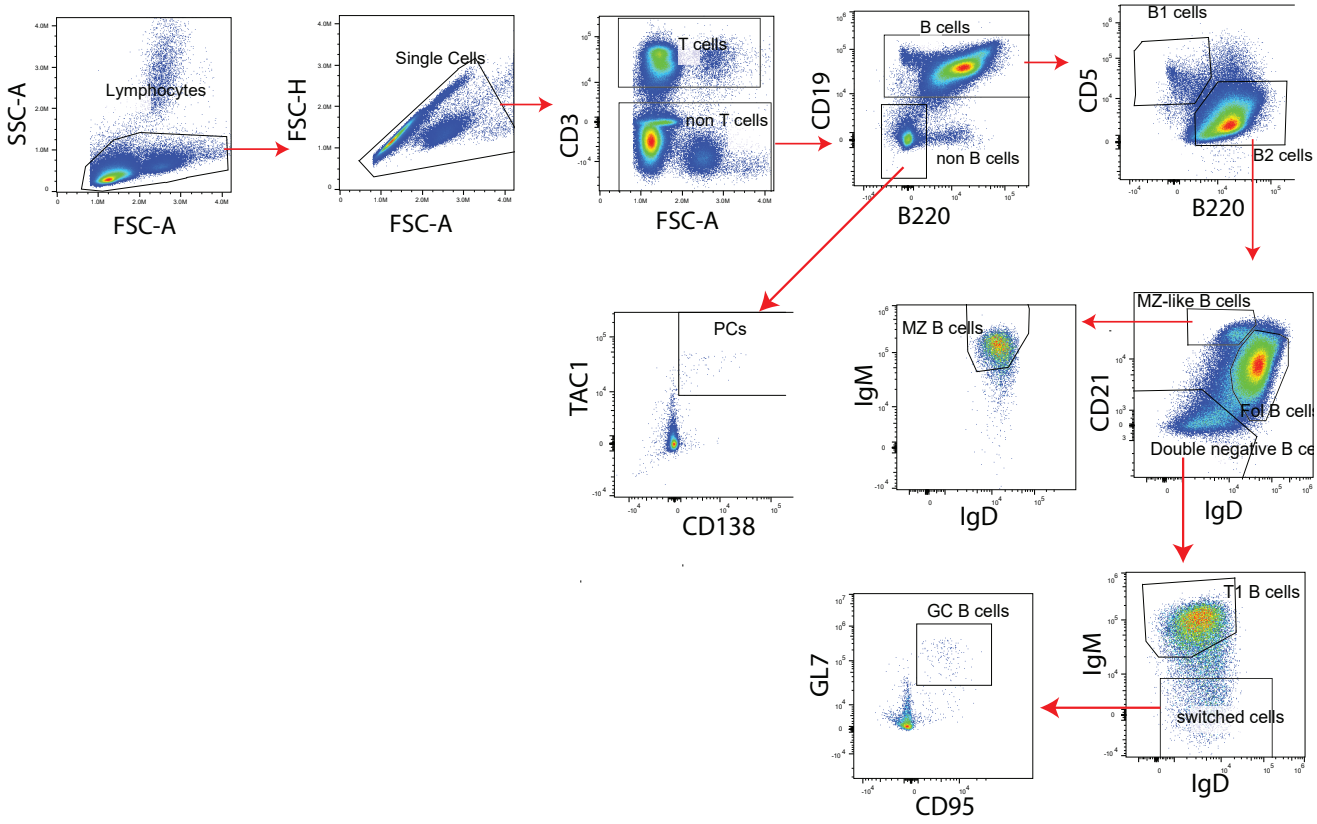

Fig. S9

Figure S9. Gating strategy for detailed B cells analysis from spleen.

Gating strategy for the flow cytometry analysis of B cell sub-sets from spleen of naïve mice after TAK-981 treatment. Data related to Fig. 5.

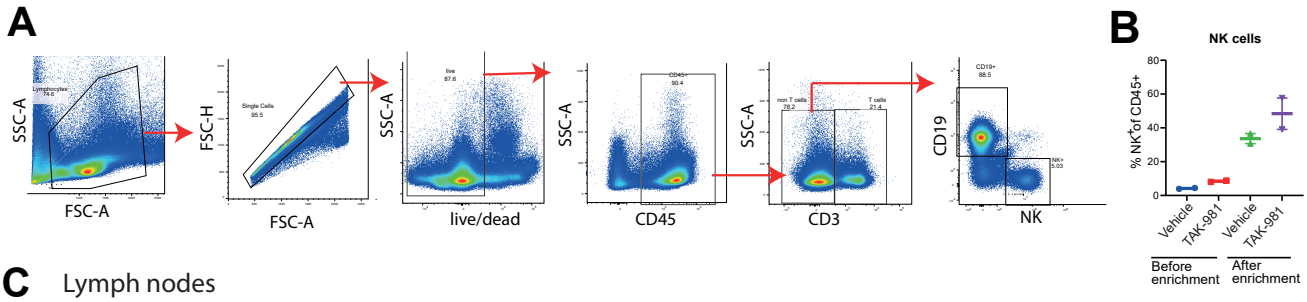

C Lymph nodes

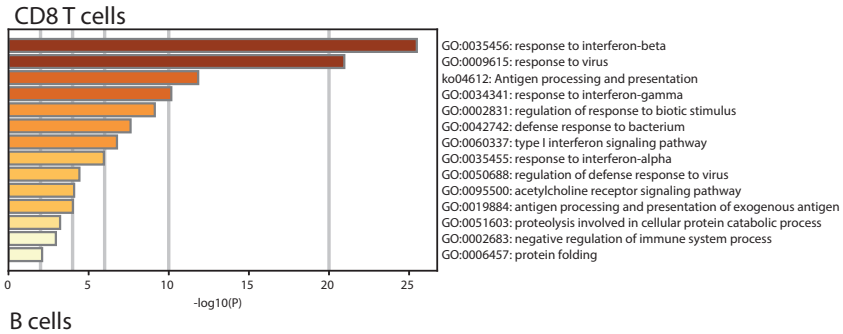

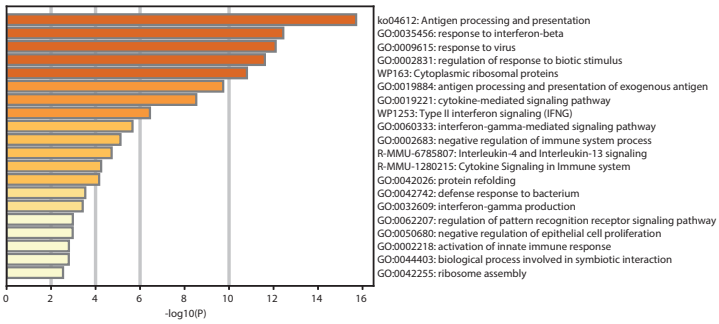

Spleen

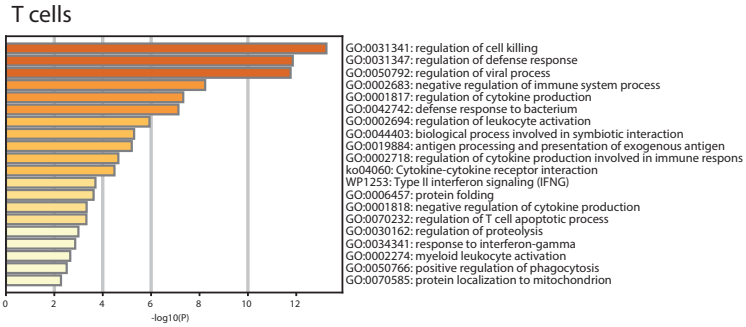

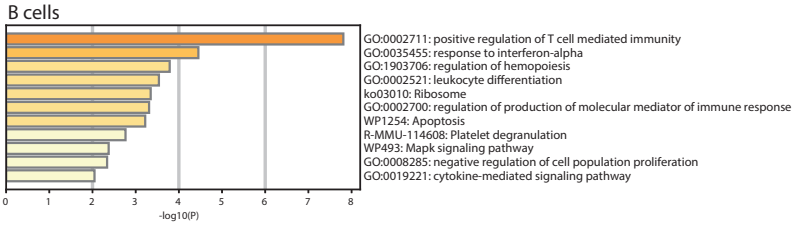

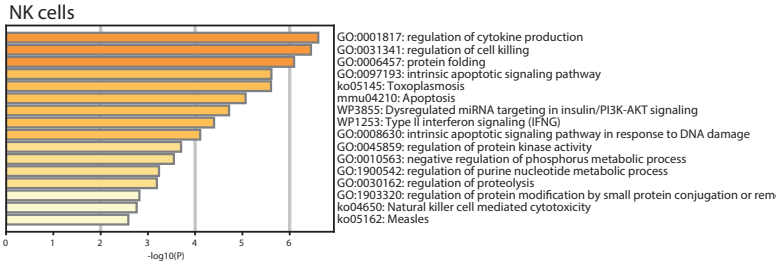

Fig. S10

Figure S10. Single cell RNA sequencing analysis.

(A) Flow cytometry gating strategy for NK cell enrichment from spleen.

(B) Graph showing NK cell enrichment in vehicle and TAK-981 treated mice (n=2).

(C) Gene ontology (GO) analysis of upregulated genes in response to TAK-981 treatment in different sets of lymphocytes from lymph nodes and spleen. Data related to Fig. 6.

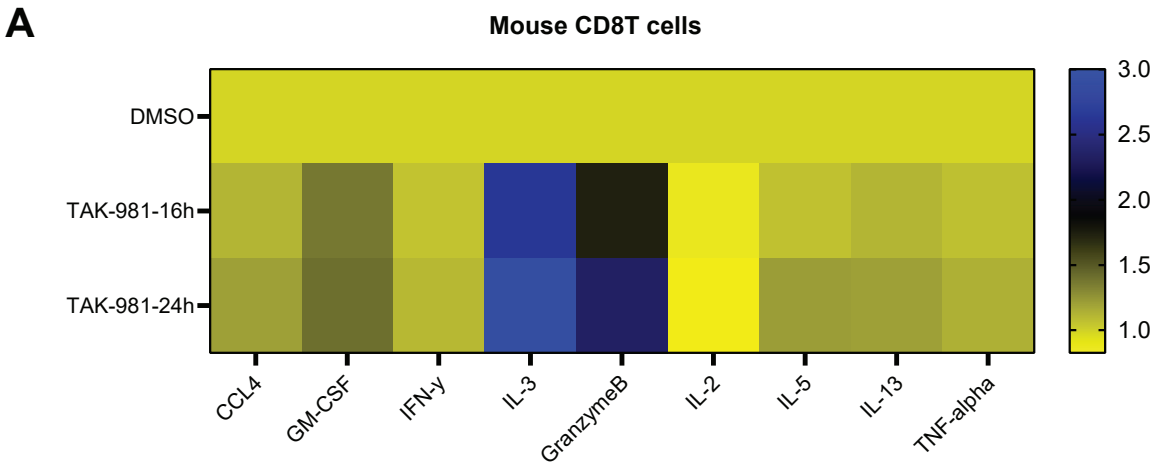
A
Mouse CD8T cells
DMSO
TAK-981-16h
TAK-981-24h
CCL4
GM-CSF
IFN-γ
IL-3
GranzymeB
IL-2
IL-5
IL-13
TNF-alpha
3.0
2.5
2.0
1.5
1.0

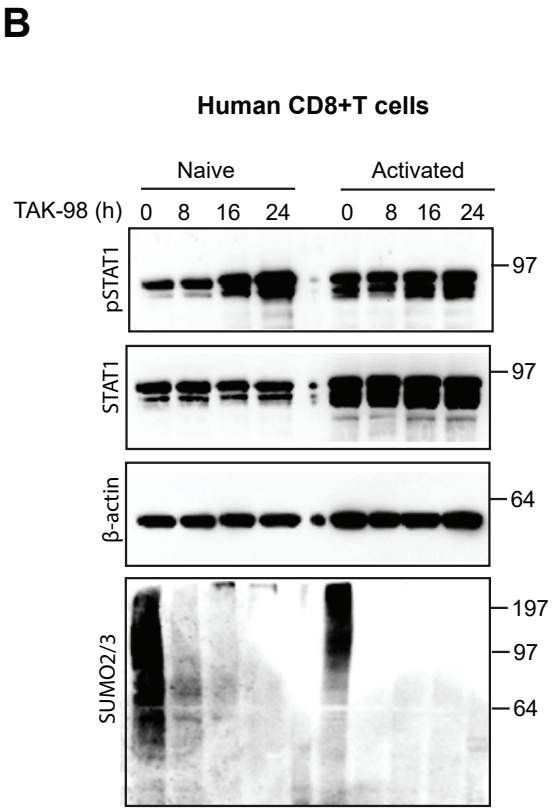
B
Human CD8+T cells
Naive
Activated
TAK-98 (h) 0 8 16 24 0 8 16 24
pSTAT1
STAT1
β-actin
SUMO2/3
97
97
64
197
97
64

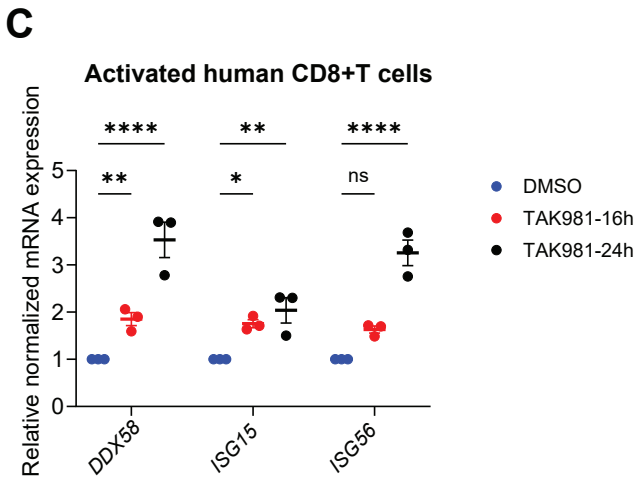
C
Activated human CD8+T cells
Relative normalized mRNA expression
****
**
**
*
****
ns
DDX58
ISG15
ISG56
DMSO
TAK981-16h
TAK981-24h

Fig. S11

Figure S11. TAK-981 activates the interferon pathway in lymphocytes.

(A) Heatmap of the relative expression of cytokines measured in cell culture medium of mouse CD8 T cells after 150 nM TAK-981 or DMSO treatment for the indicated time periods in two independent experiments.

(B) Western blot analysis showing STAT1 phosphorylation (pSTAT1) in human CD8 T cells *ex vivo* treated with 150 nM TAK-981o r DMSO control for the indicated time periods (n=2).

(C) qPCR analysis showing the expression of IFN-stimulate genes in activated human CD8 T cells treated with 150 nM TAK-981 for the indicated time periods. Statistical testing was performed using 2 way ANOVA with Dunnett's multiple comparisons test. Data are shown as mean±SEM. *p < 0.05; **p < 0.01; ***p < 0.001; ****p < 0.0001. (n=3 technical replicates). Data related to Fig. 7.

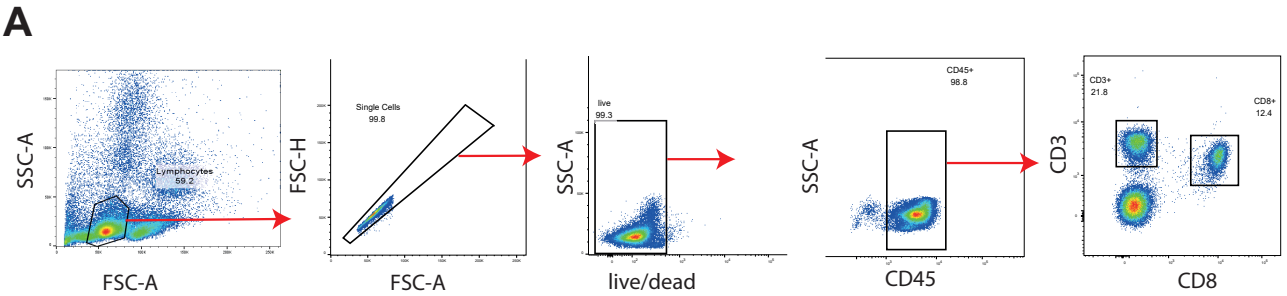
A
SSC-A
FSC-A
Lymphocytes
69.2
FSC-H
FSC-A
Single Cells
99.8
SSC-A
live/dead
live
99.3
SSC-A
CD45
CD45+
98.8
CD3
CD8
CD3+
21.8
CD8+
12.4

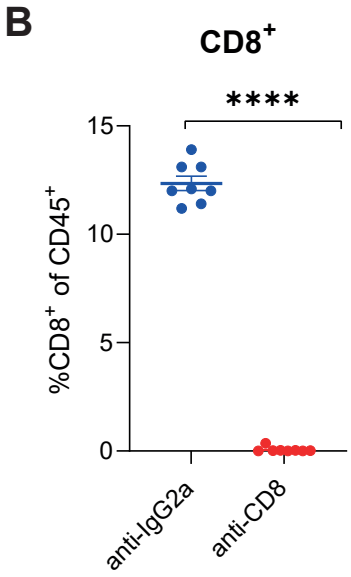
B
CD8+
****
%CD8+ of CD45+
15
10
5
0
anti-IgG2a
anti-CD8

Fig. S12

Figure S12. CD8 depletion in KPC3 tumor bearing mice.

(A) Gating strategy for the flow cytometry analysis of CD8 cell depletion from KPC3 tumor bearing mice.

(B) Quantification of CD8 cell depletion in blood. C57BL/6 mice bearing KCP3 tumors were treated with CD8 neutralizing or isotype control antibody at days -3 and -1 via intraperitoneal injection. CD8 depletion was confirmed prior to TAK-981 treatment. Dot plots represent mean and SD. Statistical testing was performed using unpaired two-tailed Welch's t test. ****$p < 0.000$. Data related to Fig. 7E.